

# The contribution of waste in the construction of composite materials

V.G. Karayannis\*, A.K. Moutsatsou

*School of Chemical Engineering, National Technical University of Athens (NTUA), 9, Iroon Polytechniou Str., 15773 Athens, Greece*

Available online 5 July 2006

## Abstract

(3Ni + Fe)–Al<sub>2</sub>O<sub>3</sub> and Ni<sub>3</sub>Fe–Al<sub>2</sub>O<sub>3</sub> composites were constructed using Ni, Fe and Ni<sub>3</sub>Fe powders (μm), recovered from metallic waste (ferrous scrap) by a hydrometallurgical process, along with a 0–35 wt.% of commercial α-Al<sub>2</sub>O<sub>3</sub> powder (0–55 vol.% theoretically). Established PM fabrication processes were applied. The successfully prepared metal–ceramics were characterized, and measurements of their physico-mechanical properties were conducted. The composite microstructures exhibit a residual porosity varying with the percent ceramic content and influenced by a certain degree of agglomeration revealed in the ceramic phase as well as by use of fabrication additives. When increasing percent ceramic amount, the composite materials become lighter, harder, stiffer and slightly stronger, while remaining conductive, although their electrical resistivity increases. Due to differences in matrix composition, Ni<sub>3</sub>Fe–Al<sub>2</sub>O<sub>3</sub> composites prevail over the (3Ni + Fe)–Al<sub>2</sub>O<sub>3</sub> ones in hardness, and slightly in stiffness and strength, at each percent ceramic content.

© 2006 Elsevier Ltd. All rights reserved.

**Keywords:** Al<sub>2</sub>O<sub>3</sub>; Composites; Microstructure-final; Powders-chemical preparation; Scrap

## 1. Introduction

Metal–ceramics show often enhanced properties, and therefore present a lot of advantages, over the unreinforced metallic materials.<sup>1–3</sup> Ceramic particle reinforced metal or alloy matrix composites in particular, have the advantage of generally being isotropic. Particulate reinforcement is also attractive as it is easier to produce and process than other existing reinforcement geometries. Successful commercial applications of this class of composites have emerged in the last years and the market is expected to expand considerably in the near future. However, among the main factors holding back more widespread commercial adoption of metal or alloy matrix composites (MMCs or AMCs, respectively) are the high cost associated with the processing and a clear decrease in ductility of the material.<sup>4</sup>

In the present research, the challenge of developing such composites while reducing their production cost led to the use of lower cost metal and alloy powders recovered from ferrous scrap, a largely available and low price waste material, in the construction of MMCs and AMCs, respectively, through established, simple and economical powder metallurgy techniques.

The apparent environmental aspects of this attempt must be emphasized here. The recovery of the matrix materials used in the composites development was realized by a hydrometallurgical process recently developed, with many advantages in its steps.<sup>5–7</sup> According to this method, Ni and Fe powders are produced by reduction with hydrogen of the Ni and Fe chlorides, respectively, which result from dissolution of the metallic waste with HCl<sub>aq</sub> and then are selectively extracted from their acidic solution by only one extractant (Versatic acid 6, Shell Company Ltd.) and finally crystallized. Ni<sub>3</sub>Fe alloy powder production is also achieved from the Ni and Fe chlorides mixtures of the same origin through similar route.

So-produced Ni powder has already been applied to Ni–Al<sub>2</sub>O<sub>3</sub> MMCs elaboration with encouraging results,<sup>8,9</sup> suggesting the investigation of a similar construction of powder-based Ni alloy matrix composites, expecting an improved behavior. P/M Ni alloys are generally known for their improved properties over conventional cast and wrought alloy products. Ni–Fe alloys have recently attracted much attention due to their interesting mechanical and magnetic properties.<sup>10</sup> Ni<sub>3</sub>Fe in particular, also exhibits a high ductility and an insensitivity towards the testing environment,<sup>11</sup> while there are ordering tendencies near this alloy composition, generally improving mechanical performance. Y<sub>2</sub>O<sub>3</sub> reinforced Ni<sub>3</sub>Fe matrix composites have already been elaborated starting from Ni and carbonyl Fe powders by Bose et al.<sup>12</sup> In the present work, Ni<sub>3</sub>Fe recovered from

\* Correspondence to: Ipirou 137 b', 41223 Larissa, Greece.

Tel.: +30 210 7723263; fax: +30 2410 286340.

E-mail address: [vkaryan@teilar.gr](mailto:vkaryan@teilar.gr) (V.G. Karayannis).

metallic waste in powder form is the raw material (instead of the elemental powders) used in the fabrication of  $\text{Ni}_3\text{Fe}$ -ceramic composites, a novel approach. Commercial grade  $\alpha\text{-Al}_2\text{O}_3$  powder was selected as the ceramic reinforcement, given the aim of retaining a lower composites production cost.  $\alpha\text{-Al}_2\text{O}_3$  is the most commonly used oxide for the production of MMCs due to its high hardness and specific stiffness, low density, electrical resistivity and coefficient of thermal expansion, and its stability providing oxidation and corrosion resistance as well as high temperature mechanical properties. It must also be noticed here, that if the development of composites starting from the elemental metal powders (Ni, Fe) with a performance comparable to this of the alloy( $\text{Ni}_3\text{Fe}$ )-powder-based ones was feasible, the use of the metal powders mixture would be preferable to the corresponding alloy powder, from an economical point of view, taking into consideration the intrinsic parameters of the above mentioned powder production method employed. For this reason,  $(3\text{Ni} + \text{Fe})\text{-Al}_2\text{O}_3$  composites were also fabricated in the present study from waste recovered Ni and Fe powders in the appropriate mixture weight ratio of 3:1, and are compared to those prepared starting from the  $\text{Ni}_3\text{Fe}$  alloy powder, not only from microstructural but also from physico-mechanical properties aspects.

## 2. Experimental

### 2.1. Materials

Ferrous scrap consisting of discarded cutting tools, that can be classified as stainless steel 316,<sup>6,9</sup> was the starting metallic waste that yielded metal and alloy powders for use in metal–ceramics in the present work. This waste material was cut into smaller pieces and then treated by the aforementioned hydrometallurgical process. The characteristics of the produced and then used Ni, Fe and  $\text{Ni}_3\text{Fe}$  powders are listed in Table 1. It can be seen that their values are generally similar to these of typical commercially available powders produced by atomization.

Commercial  $\alpha\text{-Al}_2\text{O}_3$  powder (corundum, 0.9  $\mu\text{m}$  mean particle size, 99% purity) from Aldrich Chemical Company, Inc. was selected as the ceramic reinforcement.

### 2.2. Composites

$\text{Ni}_3\text{Fe}\text{-Al}_2\text{O}_3$  and  $(3\text{Ni} + \text{Fe})\text{-Al}_2\text{O}_3$  composite specimens with a 0–35 wt.%  $\alpha\text{-Al}_2\text{O}_3$  content ( $\sim 0\text{--}55$  vol.% theoretically) were fabricated using powder metallurgy techniques: The alloy or metal powders, respectively, were dry mixed with the  $\text{Al}_2\text{O}_3$  powder, and the mixtures were uniaxially cold pressed to form a series of disc-shaped specimens. Compaction difficulties concerning compacts integrity and strength in the samples with the higher percent ceramic were observed. At the maximum pressure value of 750 MPa however, the green strength required to ensure safe handling of all prepared  $(3\text{Ni} + \text{Fe})\text{-Al}_2\text{O}_3$  samples in the subsequent fabrication steps was achieved, avoiding addition of lubricant or other compaction aid. This is generally accepted as an advantage, because additives place an upper limit on the final product densification degree that can be achieved after their removal during the compacts heating.<sup>13</sup> On the other hand, when combining  $\text{Al}_2\text{O}_3$  with  $\text{Ni}_3\text{Fe}$ , a permalloy, thus harder than Ni and Fe powders, the mixtures appeared less sensitive to the increased compaction load. To overcome these difficulties, the incorporation of 2 wt.% zinc stearate powder in the alloy–ceramic mixtures as a lubricant was selected, as compaction pressures even greater than those employed would be economically difficult to obtain. For measuring the Young's modulus and strength in particular, cylindrical composite bars were also formed, using CIP (2000 bar). In that case, polypropylene carbonate was added in the mixtures as a binder. All compacts were preheated at 400 °C for 1 h for the additives decomposition and then sintered at 1200 °C for 4 h in  $\text{N}_2$  atmosphere. The sintering time and the relatively moderate sintering temperature were selected after optimization, in order to achieve the best possible sintering results with the used simple fabrication technique while restricting an exceeding matrix grain growth and avoiding formation of brittle interfacial reaction products which, otherwise, could result in a weak interface bond.<sup>14</sup> Finally, the specimens were gradually cooled to room temperature also in  $\text{N}_2$  atmosphere, to minimize oxidation and quenching.

Phase identification of the sintered specimens was performed by X-ray diffraction (XRD) measurements (Siemens, Diffractometer D 5000). The microstructural characterization of the

Table 1  
Comparison of Ni, Fe and  $\text{Ni}_3\text{Fe}$  powders recovered from ferrous scrap with typical commercial grades

	Ni powder		Fe powder		$\text{Ni}_3\text{Fe}$ powder	
	Commercial grade (atomization) <sup>a</sup>	Recovered from scrap	Commercial grade (atomization) <sup>a</sup>	Recovered from scrap	Commercial grade (atomization) <sup>b</sup>	Recovered from scrap
Specific gravity ( $\text{g}/\text{cm}^3$ )	8.63	8.83	7.81	7.70	8.53	8.41
Specific surface ( $\text{cm}^2/\text{g}$ )	3100	3500	2500	1500		
Granulometry ( $\mu\text{m}$ )	–125 + 56:44% –56:56%	–125 + 56:28% –56:72%	–90:100%	–200:60% –90:30%	–100 mesh	–125 + 56:30% –56:70%
Particle shape	Hexagonal	Angular	Spherical	Spherical	Spherical	Angular
Apparent density ( $\text{g}/\text{cm}^3$ )			3.93	3.35		
Purity		99.9%		99.86%		99.85%

<sup>a</sup> INCO SA.

<sup>b</sup> ALFA AESAR (Ni–Fe: 80–20 wt.%).

samples was realized by light optical microscopy (Olympus, BX60M) as well as scanning electron microscopy (SEM) (JEOL JSM-6400) coupled with Energy Dispersive X-ray Spectroscopy (EDS) analysis. The green density was estimated from mass and volume of the compacts whereas the final density of the sintered samples was measured by the Archimedes' method. Then, relative densities were calculated using theoretical densities of the individual constituents. Electrical resistivity measurements were conducted on polished samples at room temperature using a four-point probe method (Programmable Current Source 224, Keithley UK; Multimeter 2000, Keithley UK; Sample rod SRH 9, Oxford Instruments UK). Hardness was measured on samples (ground and polished with SiC papers of decreasing grit size) using a Vickers microindenter (Shimadzu). Care had to be taken during specimen preparation so as to avoid significant work hardening of the surface. The mean hardness values were calculated over five valid indentations per specimen. All measurements were performed on 10 specimens of each composition and the average values were reported in the results. The Young's modulus and fracture strength were determined from bend measurements conducted on rectangular bars – machined from the fabricated cylindrical ones and then ground and polished on the tensile surface – in a load frame (Instron), using a three-point bend configuration with a crosshead speed of 0.1 m/min. The initial portion of the loading curve was used for the Young's modulus determination. All samples were finally loaded to failure, except for the pure metallic (100%) ones for which the plastic deformation exceeded 2%.

### 3. Results and discussion

#### 3.1. Compaction

The compacts before sintering were generally homogeneous. However, as it was revealed from their microstructural examination, some agglomerates existed in the ceramic phase, that can, at least partly, be attributed to the wide particle size as well as specific gravity differences between the used metal powders from metallic waste treatment and the fine commercial  $\text{Al}_2\text{O}_3$ , two factors that strongly influence the blendability of the powders during dry mixing procedures.<sup>3,15</sup> Naturally, it is difficult to achieve a homogeneous mixture during blending<sup>2</sup> and a certain degree of agglomeration is usually expected in this type of materials through a powder metallurgical fabrication route. A relative green density decreasing from 77.5 to 63.8% with the ceramic content increase from 0 to 35 wt.% for the  $(3\text{Ni} + \text{Fe})\text{-Al}_2\text{O}_3$  and 80.9 to 67.1% for the  $\text{Ni}_3\text{Fe-Al}_2\text{O}_3$  compositions, respectively, was determined. Thus, porosity was relatively restricted at this fabrication step and therefore the packing density can be considered as quite satisfactory. The angular shape of the Ni and  $\text{Ni}_3\text{Fe}$  particles may act as a contributing factor in the green strength of the pressed powders due to particle interlocking.<sup>16</sup> The difference in particle sizes for the metallic powders versus the fine ceramic has also been reported as another parameter leading to more efficient particle packing.<sup>17</sup>

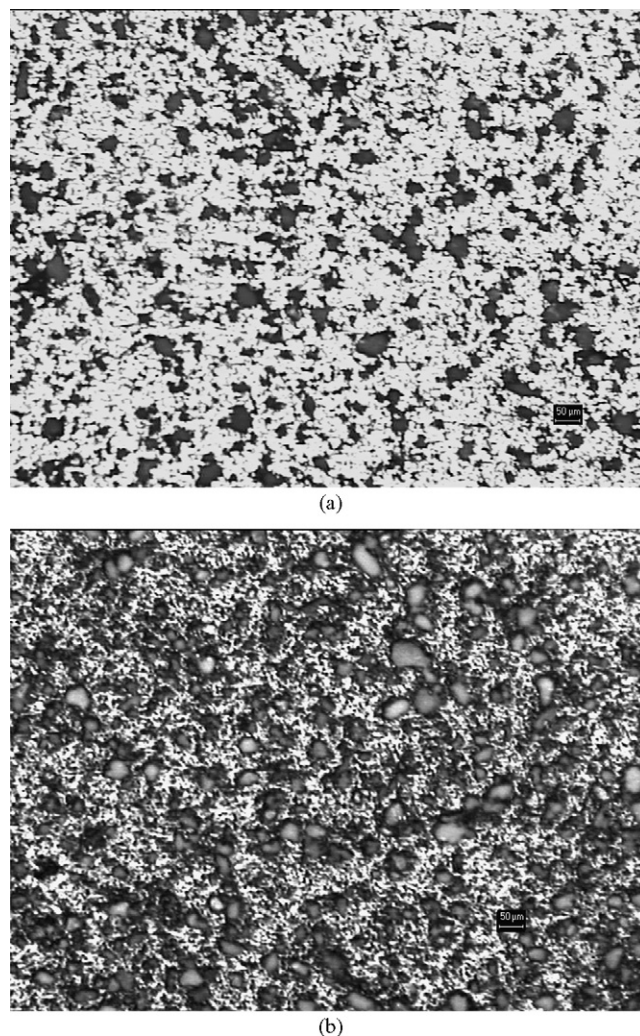


Fig. 1. Optical micrographs of 10 wt.% (a) and 20 wt.% (b) ceramic content (theoretically 19.2 and 34.9 vol.%, respectively)  $(3\text{Ni} + \text{Fe})\text{-Al}_2\text{O}_3$  MMCs.

#### 3.2. Sintering

The XRD analysis results showed that no phases other than the constituent were developed in the sintered composites, which was expected, taken into account the sintering conditions selected.

Optical micrographs of 10 and 20 wt.% ceramic content sintered  $(3\text{Ni} + \text{Fe})\text{-Al}_2\text{O}_3$  metal–ceramics are shown in Fig. 1. In these micrographs, lighter phase is the matrix and darker the  $\text{Al}_2\text{O}_3$  reinforcement. The composite microstructures consist of a continuous metal matrix reinforced with  $\text{Al}_2\text{O}_3$ . Densification occurs by atomic diffusion between particles of each metal during sintering, given that the metallic and the ceramic phase remain separate, because of lack or very limited interdiffusion of the matrix materials with the  $\text{Al}_2\text{O}_3$ . The high chemical purity of the used metal powders recovered from metallic waste, along with their relatively small particle size giving a higher surface/volume ratio and therefore an increased specific surface energy, are considered to contribute to facilitating of sintering and binding of matrix at the relatively moderate temperatures chosen in the present work, taken into consideration the simplic-



ity of the used fabrication technique. Very limited connectivity can be suggested in the ceramic phase at the applied sintering temperatures. The  $\text{Al}_2\text{O}_3$  discrete particles or agglomerates are generally uniformly distributed in the metallic matrix, located at its grain boundaries. Small isolated pores are present in the matrix. Some greater and more interconnected pores or gaps also appear, mainly located at the metal–ceramic interface of the  $(3\text{Ni} + \text{Fe})\text{--Al}_2\text{O}_3$  composites. The presence of such interfacial porosity is more intense in the regions where the  $\text{Al}_2\text{O}_3$  forms agglomerates, that points out the role of the ceramic phase local inhomogeneity in the void nucleation and growth. It should be noticed however, that a part of the porosity evident in these micrographs can be attributed to particle pullout during samples preparation for metallographic observation.<sup>18</sup>

Apparently, the lower the amount of ceramic particles, the more continuous the contact between the metallic ones, leading to a variation in consolidation degree with percent  $\text{Al}_2\text{O}_3$  amount. Actually, porosity levels increasing from 13.3 to 32.3% with the ceramic content increase from 0 to 35 wt.% (theoretically 0–53.6 vol.%, respectively) were determined in the sintered  $(3\text{Ni} + \text{Fe})\text{--Al}_2\text{O}_3$  specimens. In the sintered  $\text{Ni}_3\text{Fe}$ -based AMCs in particular, a further increase in the final porosity was measured, ranging from 18.5 to 40.9% with the ceramic content increase from 0 to 35 wt.% (theoretically 0–60.6 vol.%, respectively). These results lead to the conclusion that the lubricant, which had been necessary for facilitating compression of this group of composites, although incorporated in a weight fraction of only 2 wt.%, did not only filled existing pores during compaction, but occupied a significant volume in these materials, thus creating new pores after its removal during the compacts heating. This impact of lubricant addition is illustrated in Fig. 2, that provides SEM micrographs of 10, 20 and 30 wt.% ceramic content  $\text{Ni}_3\text{Fe}\text{--Al}_2\text{O}_3$  composites.

It can also be seen in Fig. 2, that the alloy, the darker phase according to EDS analysis results (Fig. 3), is covered by  $\text{Al}_2\text{O}_3$  particles and fine  $\text{Al}_2\text{O}_3$  dust (lighter phase). This dust could have been generated during the powders dry mixing due to wear abrasion, as demonstrated in other research on particulate MMCs where similar mixing procedures were applied.<sup>19</sup> This masking of the matrix material with fine ceramic appears to hinder sintering and therefore it can be considered as another reason for the increased porosity revealed. From an economical aspect, a cost reduction is expected by producing objects of a reduced relative density. Besides, a porous microstructure offers advantages for specific applications, e.g. with regard to thermal shock resistance due to the improved expansion tolerance and a certain decrease in the modulus of elasticity.

In Fig. 4a, apparent density of the sintered specimens decreases as the percent amount of  $\text{Al}_2\text{O}_3$  in the composites increases due to the lower density of the ceramic versus the metallic constituent. The obtained values are even lower than those theoretically expected according to the rule of mixtures, because of residual porosity.

The relationship between the electrical resistivity of the composites and the wt.%  $\text{Al}_2\text{O}_3$  content is depicted in Fig. 4b. The effect of incorporating only 10 wt.% (~20 vol.%) non-conductive ceramic phase on the composites resistivity is rel-

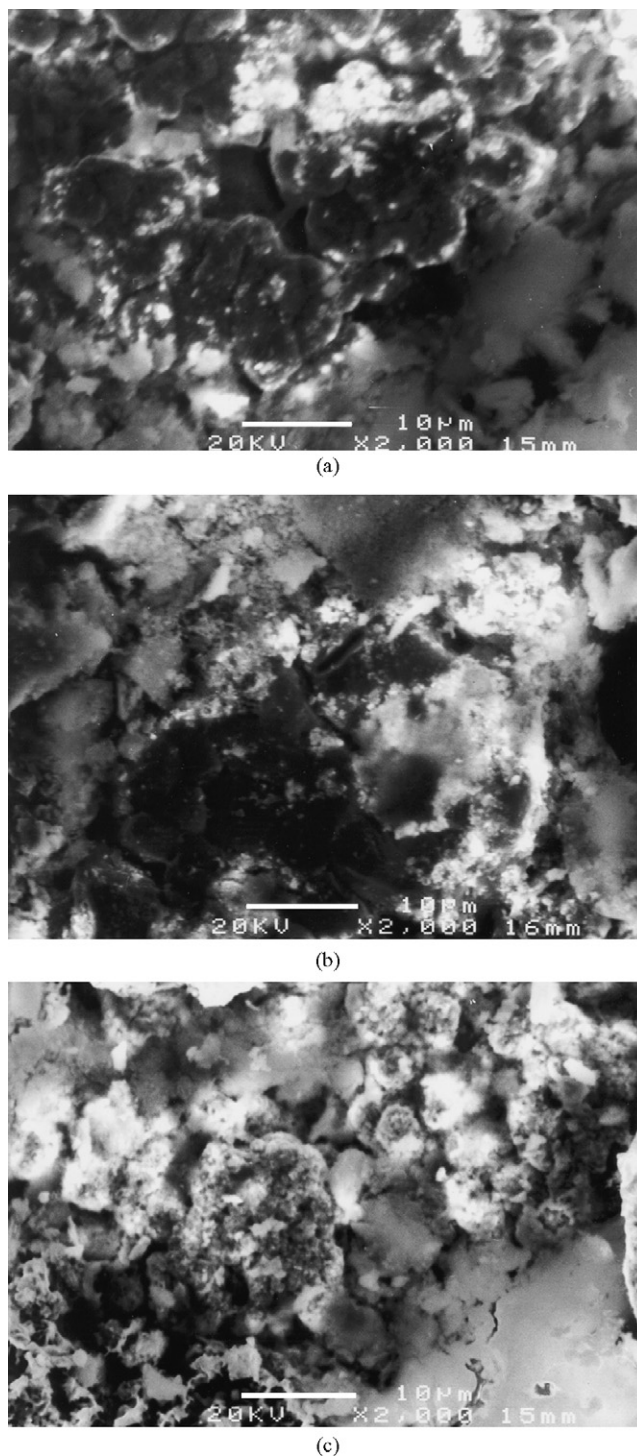


Fig. 2. SEM micrographs of  $\text{Ni}_3\text{Fe}\text{--Al}_2\text{O}_3$  composites with a 10 wt.% (a), 20 wt.% (b) and 30 wt.% (c)  $\text{Al}_2\text{O}_3$  content (theoretically 24.1, 41.7 and 55.1 vol.%, respectively).

atively restricted, but above this percent reinforcement there is a clear trend of increase in resistivity. Actually, the embedded ceramic particles behave like porosity to the passage of electric current. All fabricated composites, even them with the higher ceramic content (35 wt.% or ~55% vol.%) remain conductive, which means that their metallic phase is continuous, verifying an accepted matrix grain connectivity degree. It should be

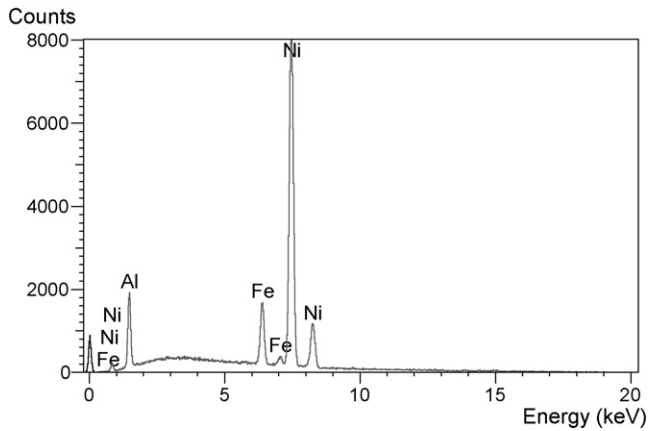


Fig. 3. Typical energy dispersive X-ray analysis spectrum (EDS) from surface (b) in Fig. 2 with a 20 wt.% ceramic content.

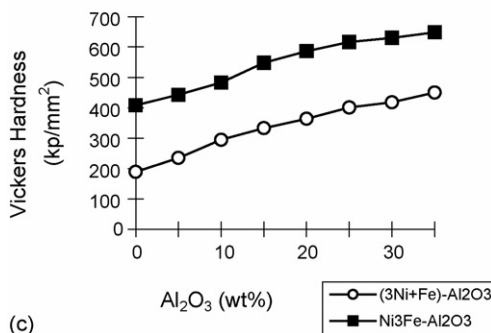
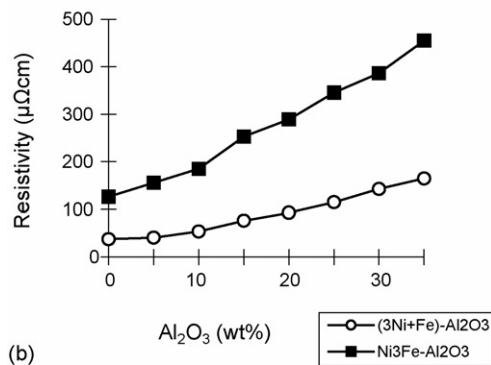
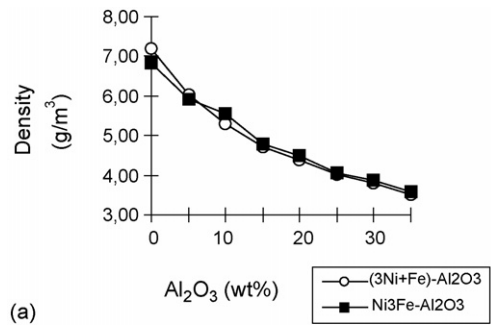


Fig. 4. Apparent density (a), electrical resistivity (b) and mean hardness (c) as a function of wt.% ceramic content.

noticed that resistivity values for the composites with the greater percent Al<sub>2</sub>O<sub>3</sub> raise at about three orders of magnitude higher than those of metals, which could be of importance for specific applications. For a better interpretation, the raise observed in the composites electrical resistivity must not only be evaluated in terms of resistivities and weight fractions of the constituent phases, but also taking into consideration some other microstructural features, including mainly the residual porosity and even a possible electron scattering due to an increased dislocation density caused in the matrix by differential thermal residual stresses due to mismatch in the thermal expansion coefficient between metallic and ceramic phase.<sup>2</sup>

When increasing percent reinforcement, the volume contiguity should also be taken into account, as the volume part of the metallic phase containing particles isolated between the insulating reinforcement prevails over the continuous (and therefore conductive) part containing interconnected metallic particles, thus impeding electron motion. On the other hand, the interfacial electrical resistance must have a negligible contribution to the overall electrical resistivity values of the composites, compared to the insulating properties of the ceramic inclusions. (3Ni + Fe)–Al<sub>2</sub>O<sub>3</sub> composites are more conductive than the Ni<sub>3</sub>Fe-based ones at each relative matrix-reinforcement composition, given a severe increase in resistivity that, generally, accompanies alloying in comparison to pure metals. Indeed, this difference becomes even more pronounced as the percent ceramic insulator increases.

The mean hardness values of the composites versus the wt.% Al<sub>2</sub>O<sub>3</sub> content are plotted in Fig. 4c. The hardening effect of the reinforcement, leading to relatively elevated hardness values at the higher percent ceramic examined, can be explained by an increase in the matrix strain hardening rate due to the development of a higher dislocation density by the presence of ceramic particles. An increase in dislocation density, resulting in further increase of matrix hardening, may also be generated in the vicinity of the Al<sub>2</sub>O<sub>3</sub> particles by the aforementioned thermal stresses developed at the metal–ceramic interfaces during and after processing. It should be noted that some variation in microhardness results was observed at each composite sample depending to indentation position. Naturally, this fluctuation is expected to a certain degree, given the large differences in the hardness of the constitutive phases. However, as this observation is more pronounced when percent reinforcement increases, it should be associated with some agglomeration in the Al<sub>2</sub>O<sub>3</sub> phase, that increase the probability of indenting the matrix away from the interface, where the beneficial effect of dislocation density is decreased. The mean hardness values achieved are clearly higher in the composites developed starting from the Ni<sub>3</sub>Fe powder, the harder of the matrix materials considered, than in the metal powder based ones, at each percent Al<sub>2</sub>O<sub>3</sub> content.

Modulus of elasticity and fracture strength of composites increase progressively with the increasing addition of stiffer Al<sub>2</sub>O<sub>3</sub> particles. This modulus increase combined with the clear decrease in density lead to an improvement of specific modulus (modulus/density), that is broadly considered as one of the most attractive features of MMCs. Naturally, this increase in stiffness is relatively restricted, mainly because of residual

porosity in the bulk of the composites and even because of some other microstructural features, such as possible microdamage accumulation in the composites during cooling, including microcracking within the  $\text{Al}_2\text{O}_3$  particles, separation of contiguous ceramic particles, or metal–ceramic decohesion, reported in other research on  $\text{Ni–Al}_2\text{O}_3$  composites.<sup>20</sup>  $\text{Ni}_3\text{Fe–Al}_2\text{O}_3$  composites slightly prevail in rigidity as well as in strength over  $(3\text{Ni} + \text{Fe})\text{–Al}_2\text{O}_3$  at a given percent reinforcement amount. The difference in stiffness of the matrix materials used and a greater heterogeneity in the metal powder based MMCs (composed from three constituents instead of only two in the case of the alloy-powder-based ones) must be responsible for these results. In fact, this heterogeneity influences significant parameters for the composites elastic behavior, including porosity, the distribution of the reinforcement particles, the nature and strength of the interface and the development of microdamages. Strengthening observed in these composites is achieved by two types of mechanisms: first, appreciable strain-induced load transfer from matrix to reinforcement, given the relatively high percent particulate ceramic content, although matrix strength maintains an important role.<sup>2</sup> Naturally, the load distribution is not expected to take place evenly between the matrix and the reinforcement due to higher stiffness of the ceramic versus the metallic phase. Secondly, strengthening mechanisms concerning the reinforcement effect on the matrix deformation (already mentioned above, discussing hardness increase) may act. Certainly, the residual porosity revealed in these materials causes fracture to occur sooner after strain localization begins. Specifically, small pores found in the matrix away from the ceramic particles reduce the composites load bearing area and therefore are detrimental to strength. Moreover, interfacial porosity, especially some greater and more interconnected pores located at the interface lead to matrix-particles debonding under lower stresses and decrease the ability of load transfer to the reinforcement, thus restricting strengthening. On the other hand, porosity is a factor restricting matrix grain growth, but the benefits of this action cannot compensate the significant effects it has on failure mechanisms. A higher relative density would normally lead to a further increase in strength but would also be more expensive to produce, and it must be noticed that for several PM applications a lower strength is not necessarily a disqualification criterion.<sup>13</sup> The homogeneity of the reinforcement distribution in the matrix may also affect strength. The agglomerates observed in the ceramic phase can be considered as sites of potential damage pre-existing to loading, because matrix regions surrounding them are subjected to higher stresses, the agglomerates not being able to support the same amount of stress as non-agglomerated particles. Therefore, stress concentration regions are introduced in the matrix leading to locally increased impedance of its plastic flow, thus affecting the composites mechanical performance, as the development and accumulation of internal microdamages during testing are more likely to occur at lower applied stresses.

#### 4. Conclusions

The construction of  $(3\text{Ni} + \text{Fe})$  matrix as well as  $\text{Ni}_3\text{Fe}$  matrix composites, reinforced with 0–35 wt.% particulate  $\text{Al}_2\text{O}_3$

(0–55 vol.% theoretically), and containing no phases other than the constituent, was achieved.

$\text{Ni}$ ,  $\text{Fe}$  and  $\text{Ni}_3\text{Fe}$  powders recovered from metallic waste (ferrous scrap), used in the present research as the raw materials along with commercial  $\alpha\text{–Al}_2\text{O}_3$ , generally showed a satisfactory behavior in the fabrication stages of the composites. Compaction facilitation by lubricant (zinc stearate powder) addition was necessary only for the composites produced from  $\text{Ni}_3\text{Fe}$  alloy powder, the harder of the matrix materials studied. After compression, satisfactory relative green density values were attained. The residual porosity determined in the sintered materials varies with the percent reinforcement amount and is influenced by some agglomeration revealed in the ceramic phase.

When percent  $\text{Al}_2\text{O}_3$  content increases, a tendency towards improved materials is exhibited, with a clear density decrease, relatively elevated hardness values and slightly increased stiffness and fracture strength. Resistivity values raise progressively at three orders of magnitude higher than those of unreinforced metals, but all composites remain conductive, even them containing the higher percent ceramic.

The lubricant demanded in the  $\text{Ni}_3\text{Fe}$ -powder-based composites in particular, although improving densification during compaction, finally leads to an increased residual porosity of the sintered composites after its removal. This increase in porosity would normally be expected to have a detrimental effect on the performance of the composites prepared from the alloy powder in comparison to the metal-powder-based ones. However, differences in matrix composition and other microstructural features compensate such an effect, finally giving a certain advantage in mechanical performance of  $\text{Ni}_3\text{Fe–Al}_2\text{O}_3$  over  $(3\text{Ni} + \text{Fe})\text{–Al}_2\text{O}_3$  composites at each percent  $\text{Al}_2\text{O}_3$  content.

#### References

1. Matthews, F. and Rawlings, R., *Composite Materials: Engineering and Science* (2nd ed.). Chapman and Hall, Oxford, 1995, p. 79.
2. Clyne, T. and Withers, P., *An Introduction to Metal Matrix Composites*. Cambridge University Press, Cambridge, 1993, pp. 347, 454.
3. Suresh, S., Mortensen, A. and Needleman, A., *Fundamentals of Metal Matrix Composites*. Butterworth-Heinemann, 1993, pp. 26, 297.
4. Mattern, A., Huchler, B., Staudenecker, D., Oberacker, R., Nagel, A. and Hoffmann, M. J., Preparation of interpenetrating ceramic-metal composites. *J. Europ. Ceram. Soc.*, 2004, **24**, 3399–3408.
5. Moutsatsou, A. and Parissakis, G., Recovery of iron, nickel, chromium and molybdenum from ferrous scrap and production at metal powders. In *Proceedings of the International Recycling Congress ReC'93, on "Advances in recovery and recycling"*, 1993, pp. 273–277.
6. Moutsatsou, A., Tsivilis, S. and Tsimas, S., Composition of complexes with  $\text{Fe(III)}$ ,  $\text{Mo(VI)}$ ,  $\text{Cr(III)}$  and  $\text{Ni(II)}$  by metal extraction with Versatic acid. *Hydrometallurgy*, 1995, **38**, 205–213.
7. Moutsatsou, A., Sotiriou, C., Tsimas, S. and Parissakis, G., Ferrous scrap, a source for the production of alloys powder by a chemical process. In *Proceedings of the International Recycling Congress ReC'97 on "Advances in recovery and recycling"*, Vol. IV, 1997, pp. 65–70.
8. Karayannis, V. and Moutsatsou, A.,  $\text{Ni–Al}_2\text{O}_3$  composites prepared using  $\text{Ni}$  powder from ferrous scrap. In *Abstracts of the Metal Matrix Composites VII Conference*, IoM, London, 1999.
9. Moutsatsou, A. K. and Karayannis, V. G., Ferrous scrap yields powders for PM and MMCs. *Metal Powder Report*, 2000, **55**, 33–36.

10. Coutu, L., Chaput, L. and Waeckerle, T., 50.50 FeNi permalloy with Ti and Cr additions for improved hardness and corrosion resistance. *J. Magn. Mater.*, 2000, **215–216**, 237–239.
11. Wang, J., Chia, W. J., Chung, Y. W. and Liu, C. T., Interaction of H<sub>2</sub>O and O<sub>2</sub> with Ni<sub>3</sub>Fe and their effects on ductility. *Intermetallics*, 2000, **8**, 353–357.
12. Bose, A., Camus, G., German, R. M., Duquette, D. J. and Stoloff, N. S., Influence of long-range order on tensile properties of Ni<sub>3</sub>Fe and Ni<sub>3</sub>Fe–Y<sub>2</sub>O<sub>3</sub> composites. *J. Mater. Res.*, 1993, **8**(3), 430–437.
13. Dowson, G., *Powder Metallurgy: The Process and its Products*. IOP Publishing Ltd, Adam Hilger, Bristol and New York, 1990, pp. 32, 46.
14. Lourdin, P., Juve, D. and Treheux, D., Nickel-alumina bonds: mechanical properties related to interfacial chemistry. *J. Europ. Ceram. Soc.*, 1996, **16**, 745–752.
15. *ASM Handbook (formerly 9th edition, Metals Handbook)-Vol. 7: Powder Metallurgy*, 5th Printing, American Society for Metals, USA, 1993. pp. 188, 192.
16. Sternowsky, S. B., O' Donnell, G. and Looney, L., Effect of particle size on the mechanical properties of SiC particulate reinforced aluminium alloy AA6061. *Key Eng. Mater.*, 1997, **127–131**, 455–462.
17. Tuan, W.-H. and Chou, W.-B., Preparation of Al<sub>2</sub>O<sub>3</sub>–AlN–Ni composites. *J. Am. Ceram. Soc.*, 1997, **80**(9), 2418–2420.
18. Bruck, H. and Rabin, B., Evaluating microstructural and damage effects in rule-of-mixtures predictions of the mechanical properties of Ni–Al<sub>2</sub>O<sub>3</sub> composites. *J. Mater. Sci.*, 1999, **34**, 2241–2251.
19. Moustafa, S. F., Abdel-Hamid, Z. and Abd-Elhay, A. M., Copper matrix SiC and Al<sub>2</sub>O<sub>3</sub> particulate composites by powder metallurgy technique. *Mater. Lett.*, 2002, **53**, 244–249.
20. Rabin, B. H., Williamson, R. L., Bruck, H. A., Wang, X.-L., Watkins, T. R., Feng, Y.-Z. *et al.*, Residual strains in an Al<sub>2</sub>O<sub>3</sub>–Ni joint bonded with a composite interlayer: experimental measurements and FEM analyses. *J. Am. Ceram. Soc.*, 1998, **81**(6), 1541–1549.